

地壳性质对滇西南锡矿床分布的约束： 基于 Hf 同位素填图

裴桐¹, 孙祥^{1*}, 郑明俊¹, 苗珂¹, 梁晓雅¹

1. 中国地质大学（北京）地球科学与资源学院，北京 100083

摘要：滇西南锡矿带是我国重要的锡成矿带之一，前人总结了滇西南锡矿带中与花岗岩相关的锡矿床的时空分布，但对锡矿床的空间展布情况与地壳性质的关系以及其控制锡成矿的原因尚不清楚。本文收集了滇西南地区已发表的早古生代-新生代花岗岩类的锆石 Hf 同位素数据，在前人对三江特提斯造山带大范围同位素填图的基础上，利用 ArcGIS 软件绘制了滇西南地区锆石 $\epsilon_{\text{Hf}}(t)$ 值和 T_{DM}^{C} 等值线图及两条典型剖面图。成图结果表明，昌宁-孟连造山带和保山地体表现为低 $\epsilon_{\text{Hf}}(t)$ 高 T_{DM}^{C} 的古老地壳特征，而腾冲地体同位素分布不均匀，既存在低 $\epsilon_{\text{Hf}}(t)$ 高 T_{DM}^{C} 的古老地壳区，又存在高 $\epsilon_{\text{Hf}}(t)$ 低 T_{DM}^{C} 的新生地壳区。滇西南地区的锡矿分布与地壳性质关系密切，锡矿均分布于低 $\epsilon_{\text{Hf}}(t)$ 高 T_{DM}^{C} 的古老地壳区，而在高 $\epsilon_{\text{Hf}}(t)$ 低 T_{DM}^{C} 的新生地壳区，尚未发现锡矿。锡矿在古老地壳区域的集中产出可能与古老富锡地壳有关。贫锡且高氧逸度地幔岩浆的混入对花岗岩中锡的富集具有抑制作用，可能是新生地壳区锡成矿作用不明显的原因。

关键词：Hf 同位素填图；地壳性质；锡矿；滇西南

中图分类号：P597; P618

收稿日期：2024-09-26

Nature of the crust constraint on tin deposit distribution in Southwest Yunnan: Based on Hf isotope mapping

Pei Tong¹, Sun Xiang^{1**}, Zheng MingJun¹, Miao Ke¹, and Liang Xiaoya¹

1. School of Earth Science and Mineral Resources, China University of Geosciences (Beijing), Beijing 100083, China

Abstract: The Southwest Yunnan Tin Belt is one of the most important tin metallogenic belts in China. The temporal and spatial distribution of granite-related tin deposits in the Southwest Yunnan Tin Belt has been summarized, but the relationship between the spatial distribution of tin deposits and the nature of the crust, as well as the reasons for controlling tin mineralization, are still unclear. In this paper, published zircon Hf isotope data of Early Paleozoic-Cenozoic granites in southwest Yunnan are collected. Based on previous large-scale isotope mapping of the Sanjiang Tethys orogenic belt, the $\epsilon_{\text{Hf}}(t)$ value and T_{DM}^{C} contour maps and two typical profiles in southwest Yunnan are drawn by ArcGIS software. The mapping results show that the Changning-Menglian orogenic belt and Baoshan terrane are ancient crustal domains with low $\epsilon_{\text{Hf}}(t)$ high T_{DM}^{C} , while the Tengchong terrane has uneven isotopic distribution, and there are both ancient crustal regions with low $\epsilon_{\text{Hf}}(t)$ and high T_{DM}^{C} , as well as newly formed crustal regions with high $\epsilon_{\text{Hf}}(t)$ and low T_{DM}^{C} . The distribution of tin deposits in southwestern Yunnan is closely related to crustal properties. Tin deposits are all distributed in ancient crustal areas with low $\epsilon_{\text{Hf}}(t)$ and high T_{DM}^{C} , while no tin deposits have been found in the newly formed crustal areas with high $\epsilon_{\text{Hf}}(t)$ and low T_{DM}^{C} . The

基金项目：国家自然科学基金重大研发计划重点支持项目 (No. 92162215); 高等学校学科创新引智计划 (No. BP0719021).

作者简介：裴桐 (2001-), 男, 硕士研究生, 主要从事与花岗岩有关的铜锡成矿作用研究. E-mail: pei_t@qq.com, ORCID: 0009-0001-0005-7627.

***通讯作者简介：**孙祥 (1980-), 男, 教授, 主要从事铜锡等战略性矿产成矿作用与勘查评价研究. E-mail: sunxiang@cugb.edu.cn.

concentrated production of tin ore in ancient crustal regions may be related to ancient tin rich crust. The mixing of low tin and high oxygen fugacity mantle magma has an inhibitory effect on the enrichment of tin in granite, which may be the reason for the unclear tin mineralization in the newly formed crustal area.

Key words: Hf isotope mapping; Nature of the crust; Tin deposit; Southwest Yunnan.

引言

锡是战略性关键金属，在航空航天、军事、芯片和新能源等领域具有重要作用（毛景文等, 2019; 蒋少涌等, 2020）。对锡矿的成矿作用、区域成矿规律及找矿勘查的研究一直是矿床学持续关注的热点（Romer and Kroner et al., 2016）。滇西南地区具有丰富的锡矿资源，它是我国重要的锡成矿带之一，前人对滇西南地区的锡矿开展了大量的成矿年代学、地球化学、成矿流体及同位素方面的研究（Chen et al., 2014; Wang et al., 2014a; Cao et al., 2016），但对于滇西南锡矿带中与花岗岩相关的锡矿床的空间展布情况、地壳性质的关系以及其控制锡成矿的原因尚不清楚。岩浆岩是探测岩石圈深部过程的“探针”，利用大量的岩浆岩同位素资料进行地体尺度的同位素填图能有效识别不同时代岩石圈成分和结构的变化，厘定区域岩石圈性质的空间展布特征，并揭示成矿系统的形成机制（莫宣学, 2011; 侯增谦和王涛, 2018）。大区域尺度的同位素填图越来越多地应用于研究岩石圈和地壳深部物质组成结构以及成矿背景等重大问题，并取得了显著进展（Hou, et al., 2015; Wang et al., 2016; 杜斌等, 2016; Deng et al., 2018; 王涛等, 2018），以上成功的案例，为本次研究提供了思路和借鉴。

本文在前人研究的基础上，收集了滇西南地区已发表的早古生代-古近纪花岗岩类锆石 Hf 同位素数据和锡石 U-Pb 定年数据，在前人对三江特提斯造山带大范围同位素填图的基础上，进一步缩小研究区域的范围，利用 ArcGIS 软件对滇西南地区开展花岗岩锆石 Hf 同位素填图，绘制典型剖面图。基于填图结果，对滇西南进行 Hf 同位素分区，揭示 Hf 同位素反映的地壳性质和锡成矿的时空关系，并与我国典型的锡成矿大省华南地区进行对比，进一步探讨地壳性质对锡成矿的控制作用。

1 区域地质背景

滇西南自东向西分为昌宁-孟连造山带、保山地体和腾冲地体（图 1）。花岗岩分布范围较广泛，与花岗岩相关的锡矿床在三者均有分布，主要分布在腾冲地体，其次为保山地体和昌宁-孟连造山带（Deng et al., 2014; Wang et al., 2016; 孙祥等, 2023）。

昌宁-孟连造山带位于保山地体和思茅地体之间，自东向西可划分为临沧花岗岩基、澜沧群和昌宁-孟连缝合带（Liu et al., 2020; Wang et al., 2021）。在昌宁-孟连缝合带的东侧发育澜沧群变质岩系和临沧花岗岩基。澜沧群由绿片岩-角闪岩相变质沉积岩和变质火山岩组成（钟大赉, 1998; Cong et al., 2021），碎屑锆石研究表明其形成时间不早于奥陶纪，其东侧被临沧岩基侵入（Wang et al., 2021; 王岳军等, 2022）。临沧岩基是三江地区出露面积最大的复式岩基，其形成与古特提斯洋俯冲和随后的碰撞造山过程有关，主体为形成于后碰撞背景的中-晚三叠世黑云母二长花岗岩，在岩基中部和南部出露高分异淡色花岗岩（Dong et al., 2013b），还有少量与俯冲相关的二叠纪花岗岩记录（Deng et al., 2018）。昌宁-孟连造山内发育的锡矿床包括勐宋、布朗山和红毛岭，锡矿多赋存在三叠纪花岗岩内部，与其周围的淡色花岗岩密切相关。勐宋、布朗山锡矿以及红毛岭锡矿分别位于临沧花岗岩基的西南部和

中部。锡石 U-Pb 年代学数据显示，锡成矿时代在 238~220Ma 之间，这些锡矿床的成矿岩体有明显的岩浆演化特征（孙祥等, 2023; Zheng et al., 2024）。

保山地体东与昌宁-孟连缝合带相邻，西与腾冲地体相接。区内出露勐统群、西盟群等变质岩系，其原被划为前寒武纪基底，但近年来的研究表明其与澜沧群类似，为一套早古生代火山-碎屑建造（Zhao et al., 2017; Wang et al., 2021）。保山地体在早古生代、三叠纪、白垩纪-古近纪以及新近纪发生多次岩浆活动及与之相关的锡成矿作用。其中，早古生代花岗岩分布在保山地体西缘（Wang et al., 2013），三叠纪花岗岩主要分布在保山地体东缘，白垩纪-古近纪花岗岩小面积分布在保山地体北部，石缸河、铁厂锡矿分布在其周缘（陆建军等, 1989; 廖世勇等, 2013），新近纪花岗岩主要沿新生代崇山-澜沧江剪切带局部发育，在西蒙地区也有出露（Zhang et al., 2010; Chen et al., 2023）。保山地体锡石 U-Pb 年代学数据显示，锡成矿作用主要发生在晚白垩世和新生代。晚白垩世锡矿典型代表为位于临沧花岗岩基西北端的松山和薅坝地，松山锡矿的成矿年龄在 79.6 ± 3.6 ~ 76.6 ± 1.5 Ma 之间，但其矿体主要产于三叠纪花岗岩及外围的早古生代变质沉积岩中，因此推测与隐伏的晚白垩花岗岩有关（Zhu et al., 2022）；薅坝地的成矿年龄为 75.5 ± 2.7 Ma，其矿体主要赋存在晚三叠碎屑岩，矿体外围出露的花岗岩形成于三叠纪，其锆石 U-Pb 年龄为 231.5 ± 3.6 Ma（Si et al., 2024）。新生代锡矿的典型代表为云岭和铁厂，云岭锡矿位于保山地体东缘的云岭花岗岩体内，其成矿年龄为 24.4 ± 0.7 Ma，含矿岩体为遭受变形的三叠纪花岗岩，其锆石 U-Pb 年龄为 231~233 Ma，矿区可能存在隐伏的晚新生代花岗岩（Xiao et al., 2024）；铁厂的成矿年龄为 31.6 ± 1.1 Ma，矿体主要产于早古生代混合岩和混合花岗岩内的构造破碎带中（Wang et al., 2024）。

腾冲地体西与西缅地体相接，东以高黎贡山剪切带为界与保山地体相邻。区内出露高黎贡群，主要由片麻岩、角闪岩、混合岩、大理岩和板岩等组成（戚学祥等, 2019），其上零星出露晚古生代-中生代沉积岩（Schwartz et al., 1995）。腾冲地体分布早古生代到新生代的花岗岩，其中以白垩纪-古近纪花岗岩为主，受到新特提斯洋俯冲和印-亚欧碰撞的控制（Deng et al., 2014; Zhu et al., 2015），早白垩世花岗岩在高黎贡山、叫鸡冠、滇滩、铁窑山、硝塘等地大面积出露，晚白垩世花岗岩在古永、三岔河、户撒等地出露，古近纪花岗岩则主要分布在那帮剪切带东西两侧（Xu et al., 2012; Xie et al., 2016）。这三期花岗岩均发育与之相关的锡矿床，且锡矿主要位于怒江断裂的西侧。早白垩世锡矿典型代表为位于腾冲地体中北部的叫鸡冠、滇滩、铁窑山等，成矿年龄在 123~118 Ma 之间，矿体多赋存于早白垩世花岗岩以及与二叠纪灰岩接触带的矽卡岩中（Chen et al., 2014）；晚白垩世锡矿的典型代表为小龙河，其位于晚白垩世古永花岗岩体东北部的小龙河岩体，成矿年龄在 73.9 ± 2.0 ~ 71.9 ± 2.3 Ma 之间，矿体主要产于同期的中细粒黑云母花岗岩 (73.9 ± 0.5 ~ 70.1 ± 0.4 Ma) 中（Chen et al., 2014）；古近纪锡矿的典型代表为来利山，成矿年龄在 52.0 ± 2.7 ~ 47.7 ± 2.0 Ma 之间，来利山锡矿与来利山复式岩体有关，其主要由早晚两阶段的花岗岩组成，而

来利山的矿体主要产于晚期的始新世花岗岩以及与二叠纪沉积岩的接触带中 (Chen et al., 2014)。

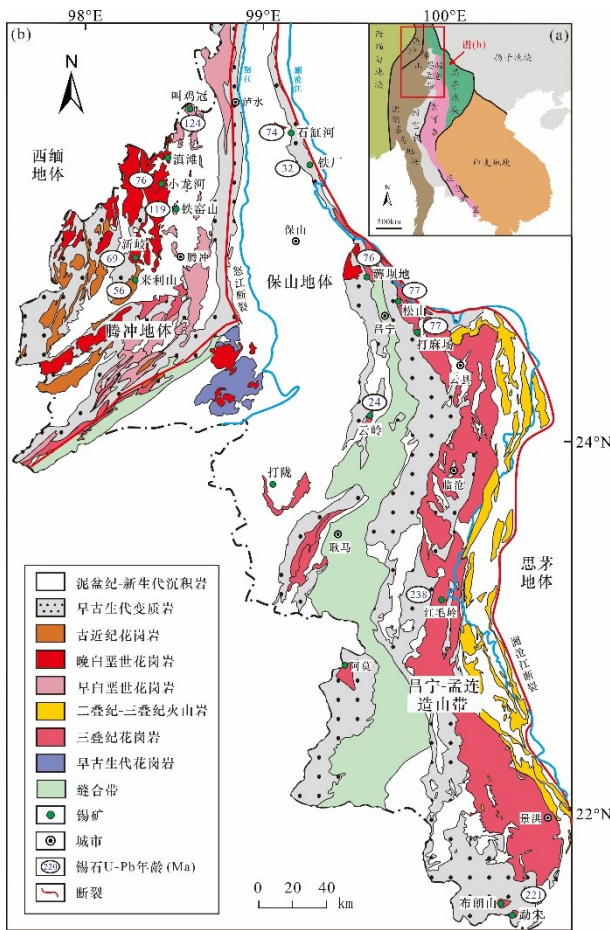


图 1 (a) 东南亚地质简图 (据 Metcalfe et al., 2021 修改); (b) 滇西南花岗岩与锡矿床分布简图 (据 Zhao et al., 2017; Wang et al., 2021; 孙祥等, 2023 修改)

Fig.1 (a) Tectonic sketch map of Southeast Asia (modified after Metcalfe et al., 2021); (b) distribution diagram of granite and tin deposits in the Southwest Yunnan (modified after Zhao et al., 2017; Wang et al., 2021; Sun et al., 2023)

2 数据来源与处理方法

锆石是岩浆岩中常见的副矿物，物理化学性质稳定，通常具有高 Hf 和低 Lu 含量，由¹⁷⁶Lu 衰变产生的¹⁷⁶Hf 极少，是进行 Hf 同位素示踪物源的理想矿物 (吴福元等, 2007; 王涛和侯增谦, 2018)。本文收集了滇西南地区 500-40 Ma 的二长花岗岩、花岗闪长岩、淡色花岗岩等酸性侵入岩的锆石 Hf 同位素数据 (共 2902 个) (腾冲数据来自李再会等, 2012; Xu et al., 2012; 林进展, 2013; Wang et al., 2013; Cao et al., 2014; Ma et al., 2014; Wang et al., 2014b; Chen et al., 2015; 林进展等, 2015; Qi et al., 2015; Wang et al., 2015c; Wang et al., 2016; Xie et al., 2016; Cao et al., 2017; Zhu et al., 2017; Cao et al., 2018; Cao et al., 2019; 保山数据来自 Chen et al., 2007; 董美玲等, 2012; 董美玲, 2013; Dong et al., 2013a; Wang et al., 2013; 禹丽等, 2014;

Zhao et al., 2014; Wang et al., 2015a; Li et al., 2016; 禹丽, 2016; Zhu et al., 2018; 昌宁-孟连造山带数据来自 Dong et al., 2013b; Yang et al., 2014; Li et al., 2015; Nie et al., 2015; Wang et al., 2015b), 并进行预处理, 使用统一的公式和参数计算每个锆石的 $\epsilon_{\text{Hf}}(t)$ 和 T_{DM}^{C} 值, 公式如下:

$$\begin{aligned}\epsilon_{\text{Hf}}(t) &= 10000 \times \left\{ \left[\frac{\left(\frac{^{176}\text{Hf}}{^{177}\text{Hf}}\right)_s - \left(\frac{^{176}\text{Lu}}{^{177}\text{Hf}}\right)_s \times (e^{\lambda t} - 1)}{\left(\frac{^{176}\text{Hf}}{^{177}\text{Hf}}\right)_{\text{CHUR},0} - \left(\frac{^{176}\text{Lu}}{^{177}\text{Hf}}\right)_{\text{CHUR}} \times (e^{\lambda t} - 1)} \right] - 1 \right\} \\ t_{\text{DM}} &= \frac{1}{\lambda} \times \ln \left[1 + \frac{\left(\frac{^{176}\text{Hf}}{^{177}\text{Hf}}\right)_s - \left(\frac{^{176}\text{Hf}}{^{177}\text{Hf}}\right)_{\text{DM}}}{\left(\frac{^{176}\text{Lu}}{^{177}\text{Hf}}\right)_s - \left(\frac{^{176}\text{Lu}}{^{177}\text{Hf}}\right)_{\text{DM}}} \right] \\ T_{\text{DM}}^{\text{C}} &= t_{\text{DM}} - (t_{\text{DM}} - t) \times \left(\frac{f_{\text{cc}} - f_s}{f_{\text{cc}} - f_{\text{DM}}} \right)\end{aligned}$$

其中, $\lambda = 1.876 \times 10^{-11}$ (Söderlund et al., 2004); $\left(\frac{^{176}\text{Hf}}{^{177}\text{Hf}}\right)_s$ 和 $\left(\frac{^{176}\text{Lu}}{^{177}\text{Hf}}\right)_s$ 为样品的标准化数据; $\left(\frac{^{176}\text{Lu}}{^{177}\text{Hf}}\right)_{\text{CHUR}} = 0.0332$; $\left(\frac{^{176}\text{Hf}}{^{177}\text{Hf}}\right)_{\text{CHUR},0} = 0.282772$ (Blichert-Toft and Albarède, 1997); $\left(\frac{^{176}\text{Lu}}{^{177}\text{Hf}}\right)_{\text{DM}} = 0.0384$; $\left(\frac{^{176}\text{Hf}}{^{177}\text{Hf}}\right)_{\text{DM}} = 0.28325$ (Griffin et al., 2000); $\left(\frac{^{176}\text{Lu}}{^{177}\text{Hf}}\right)_{\text{mean crust}} = 0.015$; $f_{\text{cc}} = \frac{\left(\frac{^{176}\text{Lu}}{^{177}\text{Hf}}\right)_{\text{mean crust}}}{\left(\frac{^{176}\text{Lu}}{^{177}\text{Hf}}\right)_{\text{CHUR}}} - 1$; $f_{\text{DM}} = \frac{\left(\frac{^{176}\text{Lu}}{^{177}\text{Hf}}\right)_{\text{DM}}}{\left(\frac{^{176}\text{Lu}}{^{177}\text{Hf}}\right)_{\text{CHUR}}} - 1$; t 为锆石形成的年龄。

随后剔除各样品中的继承锆石数据, 排除异常值所造成的干扰, 利用处理后的锆石数据计算每个岩石样品的 $\epsilon_{\text{Hf}}(t)$ 和 T_{DM}^{C} 中位数 (王涛和侯增谦, 2018)。由于每个岩石样品的数据以离散点的形式存在, 需要通过已采样点的数据来推算未采样点的值, 即栅格插值过程。插值结果将生成一个连续的表面, 在这个连续表面上可以得到每一个点的确定值。最后, 在 ArcGIS 软件中, 利用反距离权重插值法(IDW)绘制 $\epsilon_{\text{Hf}}(t)$ 和 T_{DM}^{C} 等值线图。IDW 是一种全局插值法, 它以插值点与样本点的距离为权重进行加权平均计算, 其优势是简便易操作, 不会出现无法解释的无意义结果 (李海涛和邵泽东, 2019)。

3 滇西南地区地壳性质的时空变化

滇西南地区所测量样品的 U-Pb 年龄范围约为 520-30 Ma, $\epsilon_{\text{Hf}}(t)$ 值主要在 -18 至 14 之间, 对应于约 2300-500 Ma 的地壳模式年龄 (T_{DM}^{C}) (图 2)。根据收集处理后的锆石 Hf 同位素数据生成的 $\epsilon_{\text{Hf}}(t)$ 和地壳模式年龄 (T_{DM}^{C}) 等值线图 (图 3 和图 4), 分别可以反映岩浆的可能来源和地壳源岩的形成年龄 (侯增谦和王涛, 2018; Zhang et al., 2023; Wang et al., 2023), $\epsilon_{\text{Hf}}(t) > 0$ 表明其来源于亏损地幔, 而 $\epsilon_{\text{Hf}}(t) < 0$ 表明通过部分熔融或侵蚀和沉积的过程对地壳进行了改造 (Hawkesworth et al., 2010; Belousova et al., 2010)。

在空间上， $\epsilon_{\text{Hf}}(t)$ 和 $T_{\text{DM}^{\text{C}}}$ 等值线图反映的地壳类型具有一致性，昌宁-孟连造山带和保山地体内同位素分布较均匀，主要为古老地壳；腾冲地体同位素分布则不均匀，整体上以古老地壳为主，新生地壳主要分布在腾冲地块西部。昌宁-孟连造山带内样品的 U-Pb 年龄范围约为 250-200 Ma，其同位素填图结果主要受到临沧岩基样品点的控制，其 $\epsilon_{\text{Hf}}(t)$ 范围为 -16 到 0， $T_{\text{DM}^{\text{C}}}$ 较高为 2.2-1.4 Ga，反映其主要为古老地壳的特点。保山地体的同位素填图结果受到北缘云龙花岗岩，东缘三叠纪云岭岩体，南缘西蒙花岗岩，西缘早古生代花岗岩的共同控制，其 $\epsilon_{\text{Hf}}(t)$ 范围约为 -14 至 1，具有较高的 $T_{\text{DM}^{\text{C}}}$ 范围（2.2-1.0 Ga），亦是古老地壳的结果。腾冲地体 $T_{\text{DM}^{\text{C}}}$ 年龄范围约为 2.0-0.6 Ga， $\epsilon_{\text{Hf}}(t)$ 值在 -16 至 +15 之间，大范围的 $T_{\text{DM}^{\text{C}}}$ 年龄和 $\epsilon_{\text{Hf}}(t)$ 值以及其同位素填图的结果显示出腾冲地体地壳来源的不均一性，古老地壳区域集中在那帮剪切带和大盈江断裂包围的区域内，其 $\epsilon_{\text{Hf}}(t)$ 范围为 -5 到 -13， $T_{\text{DM}^{\text{C}}}$ 范围为 1.4-2.0 Ga，而那帮剪切带以西和大盈江断裂以东区域显示出明显的高 $\epsilon_{\text{Hf}}(t)$ 值区，其 $\epsilon_{\text{Hf}}(t)$ 范围为 -3 到 5，有较低的 $T_{\text{DM}^{\text{C}}}$ 范围（0.8-1.4 Ga），表明新生地壳的贡献。

在时间上，早古生代的保山地体和腾冲地体岩浆来源主要是具有较高 $T_{\text{DM}^{\text{C}}}$ 年龄（2.3-1.6 Ga）和较负 $\epsilon_{\text{Hf}}(t)$ 值（高达 -15）的较老地壳成分。然而在白垩纪-古近纪的保山地体和腾冲地体具有广泛的 $T_{\text{DM}^{\text{C}}}$ 年龄（2.0-0.6 Ga）和 $\epsilon_{\text{Hf}}(t)$ 值（-13 至 +5），表明了古老地壳来源的异质性并且逐渐有少量新地幔成分的参与。

在 $\epsilon_{\text{Hf}}(t)$ 值和 $T_{\text{DM}^{\text{C}}}$ 等值线图的基础上，利用 ArcGIS 软件，在生成的等值线图上选择了典型剖面线 A-A' 和 B-B' 用以研究地壳性质对锡矿床的控制关系。剖面线 A-A' 为北西-南东向，自北向南穿过石缸河、铁厂、薅坝地、松山、云岭、红毛岭、布朗山、勐宋八个锡矿床。剖面线 B-B' 为北东-南西向，穿越了腾冲地体的高 $\epsilon_{\text{Hf}}(t)$ 低 $T_{\text{DM}^{\text{C}}}$ 区和低 $\epsilon_{\text{Hf}}(t)$ 高 $T_{\text{DM}^{\text{C}}}$ 区。在锆石 $\epsilon_{\text{Hf}}(t)$ 值和 $T_{\text{DM}^{\text{C}}}$ 剖面图中（图 5），连续的 $\epsilon_{\text{Hf}}(t)$ 值和 $T_{\text{DM}^{\text{C}}}$ 曲线是由计算机通过 IDW 插值形成的，表明了 $\epsilon_{\text{Hf}}(t)$ 值和 $T_{\text{DM}^{\text{C}}}$ 值沿剖面的变化情况，该曲线的插值结果受到灰色区域内样品点的控制（空心圆圈），矿床点在剖面图中的投影位置则通过其经度和围岩花岗岩的 $\epsilon_{\text{Hf}}(t)$ 值和 $T_{\text{DM}^{\text{C}}}$ 控制。

在 A-A' 剖面线中，八个锡矿床均分布在低 $\epsilon_{\text{Hf}}(t)$ 高 $T_{\text{DM}^{\text{C}}}$ 的古老地壳区域，其 $\epsilon_{\text{Hf}}(t)$ 值范围为 -4 到 -12， $T_{\text{DM}^{\text{C}}}$ 值约为 1.5-2 Ga。在 B-B' 剖面线中，来利山和新岐锡矿也均分布在低 $\epsilon_{\text{Hf}}(t)$ 高 $T_{\text{DM}^{\text{C}}}$ 的古老地壳区，其 $\epsilon_{\text{Hf}}(t)$ 值范围为 -8 到 -11， $T_{\text{DM}^{\text{C}}}$ 值约为 1.7-1.8 Ga，而在高 $\epsilon_{\text{Hf}}(t)$ 低 $T_{\text{DM}^{\text{C}}}$ 的新生地壳区，未发现锡矿。从等值线图上看，其余的锡矿床（如叫鸡冠、小龙河、西蒙等）也都分布在低 $\epsilon_{\text{Hf}}(t)$ 高 $T_{\text{DM}^{\text{C}}}$ 的古老地壳区，这表明滇西南的锡矿分布严格受到地壳性质的控制，锡矿均发育在古老地壳区域，新生地壳区域并未发现锡矿。

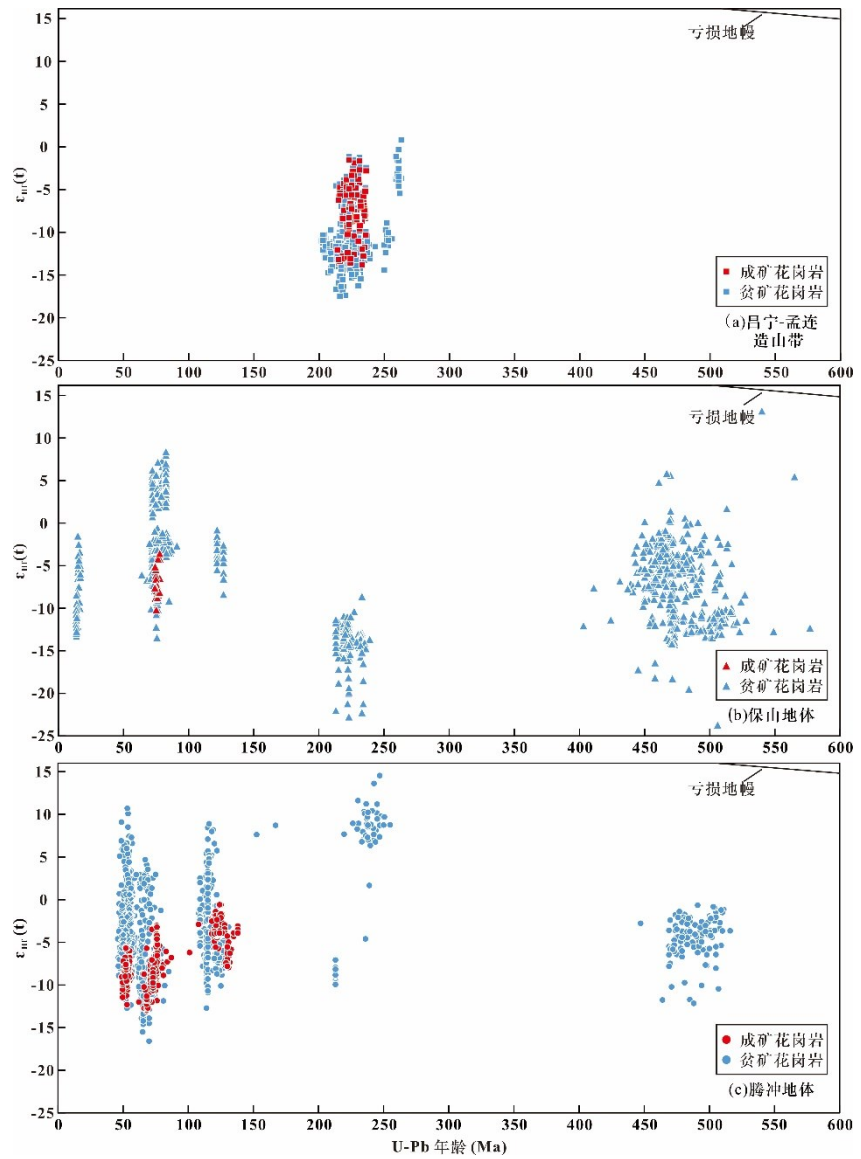


图 2 滇西南花岗岩锆石 $\epsilon_{\text{Hf}}(t)$ 与 U-Pb 年龄图

Fig. 2 Plots of $\epsilon_{\text{Hf}}(t)$ versus U-Pb ages of granite zircons in Southwest Yunnan

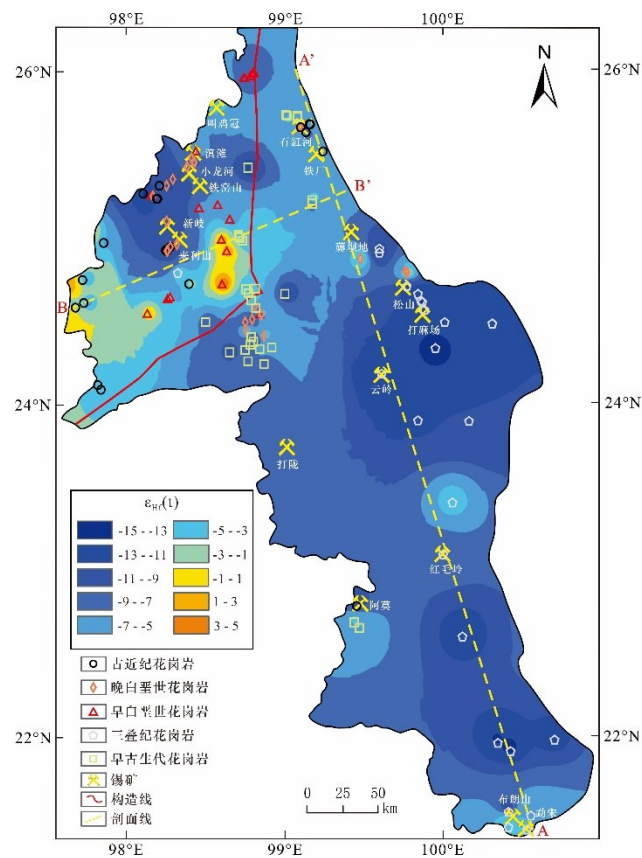


图 3 滇西南花岗岩锆石 $\epsilon_{\text{Hf}}(t)$ 等值线图

Fig. 3 Zircon $\epsilon_{\text{Hf}}(t)$ contour map of granites in Southwest Yunnan

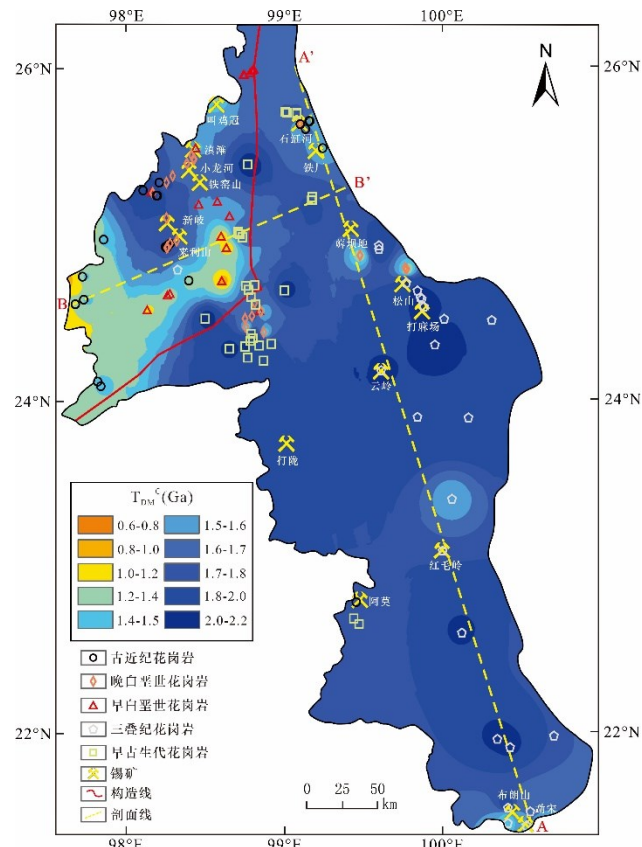


图 4 滇西南花岗岩锆石 T_{DM}^C 等值线图

Fig. 4 Zircon T_{DM}^C contour map of granites in Southwestern Yunnan

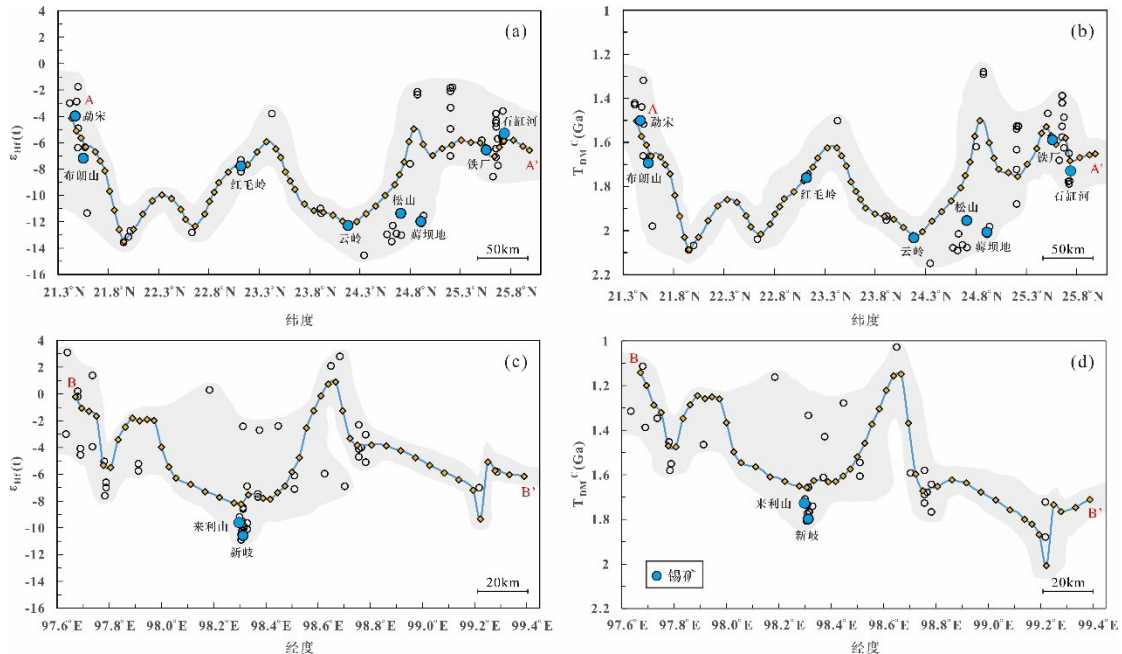


图 5 锆石 $\epsilon_{Hf}(t)$ 值和 T_{DM}^C 沿 A-A' 和 B-B' 剖面的变化

Fig. 5 Variations in zircon $\epsilon_{Hf}(t)$ and T_{DM}^C values along A-A' and B-B' profiles

4 地壳性质对滇西南锡矿床分布的约束

锡是变价元素，在还原的花岗质岩浆体系中，锡主要以 Sn^{2+} 形式存在，在岩浆结晶分异过程中不相容，因此随着岩浆结晶分异而不断在残余熔体中富集并最终形成锡矿床，而在氧化的花岗质岩浆中，锡主要以 Sn^{4+} 形式存在，在岩浆结晶分异过程中进入先形成的铁-钛氧化物和镁铁质矿物中，难以在残余熔体中富集，因此传统观点认为，锡矿的形成在岩浆过程中受到还原性花岗质岩浆结晶分异过程的控制 (Lehmann, 1990, 2021)。但近年来也有学者发现经受强烈化学风化而预富集锡的变质沉积岩通过部分熔融即可形成锡花岗岩，因此提出源岩锡的预富集对锡矿形成起控制作用 (Romer and Kroner, 2016)。

华南是世界典型的钨锡成矿大省，华南地区的花岗岩和钨锡成矿研究对该领域有很好的指导意义 (吴福元等, 2023)。华南发育多期岩浆作用，地壳改造强烈，研究发现由于华南锡矿床主要形成于白垩世，大部分矿床与中生代花岗岩有关 (Wang et al., 2020)。Zhang 等 (2023) 通过 Hf 同位素填图确定了华南地区的锡矿分布与古老地壳在空间分布上的相关性。其中，南岭成矿带中锡矿分布在同位素过渡带上 ($\epsilon_{Hf}(t) = -8$ 至 -4)，江南成矿带的锡矿多出现在 $\epsilon_{Hf}(t)$ 值适中 (-6 至 -2) 的区域，其对应的地壳性质均表现为受改造的地壳特征。对华南地区的区域地球化学调查也表明锡矿的分布和锡的地球化学异常高值区域高度一致，80%以上的矿点位于归一化地球化学丰度值大于 2 的位置 (Liu et al., 2021)。因此认为南岭成矿带和江南成矿带 Sn 的富集是多期地壳改造以及地壳源区 Sn 富集共同控制的结果 (Zhang et al., 2023)。

通过对比可以发现，滇西南地区锡矿的分布特点与华南地区类似，锡矿都主要分布于 $\epsilon_{\text{Hf}}(t)$ 值较负（-12 至 -3）的古老地壳中，而新生地壳区未发现锡矿。腾冲和保山地区的锡矿主要集中分布在北部， $\epsilon_{\text{Hf}}(t)$ 值在 -11~ -5 之间，昌宁-孟连造山带地区的锡矿主要分布在其中部和南部， $\epsilon_{\text{Hf}}(t)$ 值在 -11~ -3 之间。这些地区的地壳都受到沉积和风化控制作用，从而对锡矿分布有着一定的控制作用。从寒武纪至志留纪，临沧、保山和腾冲地体位于东冈瓦纳北缘作为大陆边缘接受沉积物的堆积（Liu et al., 2020），对这些沉积物强烈的化学风化作用可能导致 Sn、W 等元素的富集（Romer and Kroner, 2016）。通过对滇西南地区开展地层地球化学的研究发现，该区域早古生代变质岩的 Sn 含量相对于上地壳的 Sn 含量普遍较高，其中，高黎贡山群和澜沧群平均 Sn 含量大约可达到 4ppm，特别是西蒙群地层平均 Sn 含量可达平均上地壳 Sn 含量的 15 倍 (~30ppm)，（胡斌, 2002），是形成含锡花岗岩的有利来源。而在新生地壳区，如腾冲地区的中西部 $\epsilon_{\text{Hf}}(t)$ 值 (-1 至 5) 要高于与古老地壳 $\epsilon_{\text{Hf}}(t)$ 值，整体较正，在这些区域暂未发现锡矿的分布。那帮剪切带西侧和大盈江断裂东侧的高 $\epsilon_{\text{Hf}}(t)$ 低 T_{DM}^{C} 区表明亏损地幔成分的加入，在那帮发现的角闪岩和变质辉长岩 $\epsilon_{\text{Hf}}(t)$ 为 1.8-11.6 证明了亏损地幔成分的存在（Wang et al., 2014a; Zhao et al., 2019）。地幔岩浆一般贫锡（0.13 ppm, Lehmann, 2021），并且相对氧化 ($\Delta \text{FMQ}=0$ -1, Evans et al., 2012)，它在花岗质岩浆中的混合会降低锡含量，增加氧逸度，这些因素不利于锡在岩浆结晶分过程中富集（Yang et al., 2020），这可能是在腾冲高 $\epsilon_{\text{Hf}}(t)$ 低 T_{DM}^{C} 的新生地壳区，未发现锡矿的原因。

5 结论

- (1) Hf 同位素填图结果表明，在空间上，昌宁-孟连造山带和保山地体表现为低 $\epsilon_{\text{Hf}}(t)$ 高 T_{DM}^{C} 的古老地壳特征，而腾冲地体同位素分布不均匀，既存在低 $\epsilon_{\text{Hf}}(t)$ 高 T_{DM}^{C} 的古老地壳区，又存在高 $\epsilon_{\text{Hf}}(t)$ 低 T_{DM}^{C} 的新生地壳区。在时间上，从早古生代至古近纪，保山地体和腾冲地体的地壳特征由古老地壳逐渐表现为有少量新地幔成分的参与。
- (2) 通过在同位素填图结果的基础上绘制两条典型的剖面线，并将滇西南地区与典型锡成矿大省华南地区进行对比分析可以发现，锡矿分布与古老地壳在空间分布上具有相关性，即锡矿均分布于低 $\epsilon_{\text{Hf}}(t)$ 高 T_{DM}^{C} 的古老地壳区，而在高 $\epsilon_{\text{Hf}}(t)$ 低 T_{DM}^{C} 的新生地壳区域，尚未发现锡矿。锡矿在古老地壳区域的集中分布可能与古老的富锡地壳分布有关，古老富锡地壳是形成含锡花岗岩的有利来源。而新生地壳区锡矿的缺乏可能与贫锡且高氧逸度的地幔岩浆混入抑制了锡在花岗岩中的富集过程有关。

致谢

感谢两位审稿专家和编辑提出的修改意见。

References

- Belousova, E.A., Kostitsyn, Y.A., Griffin, W.L., et al., 2010. The Growth of the Continental Crust: Constraints from Zircon Hf-Isotope Data. *Lithos*, 119(3–4): 457–466.
- Blichert-Toft, J. Albarède, F., 1997. The Lu-Hf Isotope Geochemistry of Chondrites and the Evolution of the Mantle-crust System. *Earth and Planetary Science Letters*, 148(1–2): 243–258.
- Cao, H.W., Pei, Q.M., Zhang, S.T., et al., 2017. Geology, Geochemistry and Genesis of the Eocene Lailishan Sn Deposit in the Sanjiang Region, SW China. *Journal of Asian Earth Sciences*, 137: 220–240.
- Cao, H.W., Zhang, S.T., Lin, J.Z., et al., 2014. Geology, Geochemistry and Geochronology of the Jiaojiguanliangzi Fe-Polymetallic Deposit, Tengchong County, Western Yunnan (China): Regional Tectonic Implications. *Journal of Asian Earth Sciences*, 81: 142–152.
- Cao, H.W., Zhang, Y.H., Santosh, M., et al., 2018. Mineralogy, Zircon U-Pb-Hf Isotopes, and Whole-Rock Geochemistry of Late Cretaceous-Eocene Granites from the Tengchong Terrane, Western Yunnan, China: Record of the Closure of the Neo-Tethyan Ocean. *Geological Journal*, 53(4): 1423–1441.
- Cao, H.W., Zhang, Y.H., Tang, L., et al., 2019. Geochemistry, Zircon U-Pb Geochronology and Hf Isotopes of Jurassic-Cretaceous Granites in the Tengchong Terrane, SW China: Implications for the Mesozoic Tectono-Magmatic Evolution of the Eastern Tethyan Tectonic Domain. *International Geology Review*, 61(3): 257–279.
- Cao, H.W., Zou, H., Zhang, Y.H., et al., 2016. Late Cretaceous Magmatism and Related Metallogeny in the Tengchong Area: Evidence from Geochronological, Isotopic and Geochemical Data from the Xiaolonghe Sn Deposit, Western Yunnan, China. *Ore Geology Reviews*, 78: 196–212.
- Chen, F., Li, X.H., Wang, X.L., et al., 2007. Zircon Age and Nd-Hf Isotopic Composition of the Yunnan Tethyan Belt, Southwestern China. *International Journal of Earth Sciences*, 96: 1179–1194.
- Chen, X.C., Hu, R., Bi, X.W., et al., 2015. Petrogenesis of Metaluminous A-Type Granitoids in the Tengchong-Lianghe Tin Belt of Southwestern China: Evidences from Zircon U-Pb Ages and Hf-O Isotopes, and Whole-Rock Sr-Nd Isotopes. *Lithos*, 212: 93–110.
- Chen, X.C., Hu, R.Z., Bi, X.W., et al., 2014. Cassiterite LA-MC-ICP-MS U/Pb and Muscovite $^{40}\text{Ar}/^{39}\text{Ar}$ Dating of Tin Deposits in the Tengchong-Lianghe Tin District, NW Yunnan, China. *Mineralium Deposita*, 49: 843–860.
- Chen, X.C., Li, P., Mao, K.N., et al., 2023. Zircon U-Pb Ages and Hf-O Isotopes of Xiaomasa Miocene Granite in the Ximeng Area, Western Yunnan, Southwest China: Constraints on Petrogenesis and Tectonic Setting. *Geological Journal*, 58(8): 2952–2967.
- Cong, F., Wu, F.Y., Li, W.C., et al., 2021. Petrogenesis of the Main Range and Eastern Province Granites in Eastern Myanmar: New Insights from Zircon U-Pb Ages and Sr-Nd Isotopes. *Lithos*, 382: 105895.
- Deng, J., Wang, C.M., Bagas, L., et al., 2018. Crustal Architecture and Metallogenesis in the South-Eastern North China Craton. *Earth-Science Reviews*, 182: 251–272.
- Deng, J., Wang, Q.F., Li, G.J., et al., 2014. Cenozoic Tectono-Magmatic and Metallogenic Processes in the Sanjiang Region, Southwestern China. *Earth-Science Reviews*, 138: 268–299.
- Dong M.L., Dong G.C., Mo X.X., et al., 2013a. Geochemistry, Zircon U-Pb Geochronology and Hf Isotopes of Granites in the Baoshan Block, Western Yunnan: Implications for Early Paleozoic Evolution along the Gondwana Margin. *Lithos*, 179: 36–47.
- Dong, G.C., Mo, X.X., Zhao, Z.D., et al., 2013b. Zircon U-Pb Dating and the Petrological and Geochemical Constraints on Lincang Granite in Western Yunnan, China: Implications for the Closure of the Paleo-Tethys Ocean. *Journal of Asian Earth Sciences*, (62): 282–294.
- Dong, M.L., 2013. Geochemistry and Geochronology of the Early Palaeozoic Granitoids in Baoshan Block, Western Yunnan and Their Tectonic Implications (Dissertation). China University of Geosciences, Beijing (in Chinese with English abstract).
- Dong, M.L., Dong, G.C., Mo, X.X., et al., 2012. Geochronology and Geochemistry of the Early Palaeozoic

- Granitoids in Baoshan Block, Western Yunnan and Their Implications. *Acta Petrologica Sinica*, 28(05): 1453–1464, (in Chinese with English abstract).
- Du, B., Wang, C.M., He, X.Y., et al., 2016. Advances in Research of Bulk-Rock Nd and Zircon Hf Isotopic Mappings: Case Study of the Sanjiang Tethyan Orogen. *Acta Petrologica Sinica*, 32(08): 2555–2570 (in Chinese with English abstract).
- Evans, K.A., Elburg, M.A., Kamenetsky, V.S., 2012. Oxidation State of Subarc Mantle. *Geology*, 40(9): 783–786.
- Griffin, W.L., Pearson, N.J., Belousova, E., et al., 2000. The Hf Isotope Composition of Cratonic Mantle: LAM-MC-ICPMS Analysis of Zircon Megacrysts in Kimberlites. *Geochimica et cosmochimica acta*, 64(1): 133–147.
- Hawkesworth, C.J., Dhuime, B., Pietranik, A.B., et al., 2010. The Generation and Evolution of the Continental Crust. *Journal of the Geological Society*, 167(2): 229–248.
- Hou, Z.Q. Wang T., 2018. Isotopic Mapping and Deep Material Probing (II): Imaging Crustal Architecture and Its Control on Mineral Systems. *Earth Science Frontiers*, 25(06): 20–41 (in Chinese with English abstract).
- Hou, Z.Q., Duan, L.F., Lu, Y.J., et al., 2015. Lithospheric Architecture of the Lhasa Terrane and Its Control on Ore Deposits in the Himalayan-Tibetan Orogen. *Economic Geology*, 110(6): 1541–1575.
- Hu, B., 2002. Metallogeny of Copper Ores from the Lancangjiang Metallogenic Belt in Western Yunnan (Dissertation). Central South University, Hunan (in Chinese with English abstract).
- Jiang, S.Y., Zhao, K.D., Jiang, H., et al., 2020. Spatiotemporal Distribution, Geological Characteristics and Metallogenic Mechanism of Tungsten and Tin Deposits in China: An Overview. *Chinese Science Bulletin*, 65(33): 3730–3745 (in Chinese with English abstract).
- Lehmann, B., 1990. Metallogeny of Tin in Central Thailand: A Genetic Concept. *Geology*, 17(5): 426–429.
- Lehmann, B., 2021. Formation of Tin Ore Deposits: A Reassessment. *Lithos*, 402: 105756.
- Li, D.P., Chen, Y.L., Hou, K.J., et al., 2015. Detrital Zircon Record of Paleozoic and Mesozoic Meta-Sedimentary Strata in the Eastern Part of the Baoshan Block: Implications of Their Provenance and the Tectonic Evolution of the Southeastern Margin of the Tibetan Plateau. *Lithos*, 227: 194–204.
- Li, G.J., Wang, Q.F., Huang, Y.H., et al., 2016. Petrogenesis of Middle Ordovician Peraluminous Granites in the Baoshan Block: Implications for the Early Paleozoic Tectonic Evolution along East Gondwana. *Lithos*, 245: 76–92.
- Li, H.T. Shao, Z.D., 2019. Review of Spatial Interpolation Analysis Algorithm. *Computer Systems & Applications*, 28(07): 1–8 (in Chinese with English abstract).
- Li, Z.H., Lin, S.L., Cong, F., et al., 2012. U-Pb Dating and Hf Isotopic Compositions of Quartz Diorite and Monzonitic Granite from the Tengchong-Lianghe Block, Western Yunnan, and Its Geological Implications. *Acta Geologica Sinica*, 86(7): 1047–1062 (in Chinese with English abstract).
- Liao, S.Y., Wang, D.B., Tang, Y., et al., 2013. LA-ICP-MS U-Pb Age of Two-Mica Granite in the Yunlong Tin-Tungsten Metallogenic Belt in Three River Region and Its Geological Implications. *Acta Petrologica et Mineralogica*, 32(04): 450–462 (in Chinese with English abstract).
- Lin, J.Z., 2013. Geological and Geochemical Characteristics of Lailishan Granites in Tengchong Tin Belt, Western Yunnan, and Their Relation to Mineralization (Dissertation). China University of Geosciences, Beijing (in Chinese with English abstract).
- Lin, J.Z., Cao, H.W., Zhang, S.T., et al., 2015. Geochemical Characteristics and Zircon U-Pb Dating for A-Type Granites in Lailishan, Tengchong, Southeastern Tibet and Its Tectonic Significance. *Geotectonica et Metallogenesis*, 39(05):959–971 (in Chinese with English abstract).
- Liu, B.B., Peng, T.P., Fan, W.M., et al., 2020. Tectonic Evolution and Paleoposition of the Baoshan and Lincang Blocks of West Yunnan during the Paleozoic. *Tectonics*, 39(10): e2019TC006028.
- Liu, W.Q., Lü, Q.T., Cheng, Z.Z., et al., 2021. Multi-Element Geochemical Data Mining: Implications for Block

- Boundaries and Deposit Distributions in South China. *Ore Geology Reviews*, 133: 104063.
- Lu, J.J., Zhu, J.C., Liu, C.S., et al., 1989. Characteristics of Yunlong Migmatites in Western Yunnan Province and Their Relation to Tin Mineralization. *Geotectonica et Metallogenesis*, (03): 264–275 (in Chinese with English abstract).
- Ma, L.Y., Wang, Y.J., Fan, W.M., et al., 2014. Petrogenesis of the Early Eocene I-Type Granites in West Yingjiang (SW Yunnan) and Its Implication for the Eastern Extension of the Gangdese Batholiths. *Gondwana Research*, 25(1): 401–419.
- Mao, J.W., Yuan, S.D., Xie, G.Q., et al., 2019. New Advances on Metallogenetic Studies and Exploration on Critical Minerals of China in 21st Century. *Mineral Deposits*, 38(05): 935–969 (in Chinese with English abstract).
- Metcalfe, I., 2021. Multiple Tethyan Ocean Basins and Orogenic Belts in Asia. *Gondwana Research*, 100: 87–130.
- Mo, X.X., 2011. Magma and Magmatic/Igneous Rocks: A Lithoprobe into the Deep Earth and Records of the Earth's Evolution. *Chinese Journal of Nature*, 33(05): 255–259+313 (in Chinese with English abstract).
- Nie, X.M., Feng, Q.L., Qian X., et al., 2015. Magmatic Record of Prototethyan Evolution in SW Yunnan, China: Geochemical, Zircon U-Pb Geochronological and Lu-Hf Isotopic Evidence from the Huimin Metavolcanic Rocks in the Southern Lancangjiang Zone. *Gondwana Research*, 28(2): 757–768.
- Qi, X.X., Zhu, L.H., Grimmer, J.C., et al., 2015. Tracing the Transhimalayan Magmatic Belt and the Lhasa Block Southward Using Zircon U-Pb, Lu-Hf Isotopic and Geochemical Data: Cretaceous-Cenozoic Granitoids in the Tengchong Block, Yunnan, China. *Journal of Asian Earth Sciences*, 110: 170–188.
- Qi, X.X., Wei, C., Cai, Z.H., et al., 2019. Sedimentary Age of Metamorphic Rocks of Gaoligong Group in Tengchong Block, Western Yunnan and Its Relationship with Subduction/Accretion of Prototethys: Evidences from Detrital Zircon U-Pb Dating and Geochemistry. *Acta Geologica Sinica*, 93(01): 94–116 (in Chinese with English abstract).
- Romer, R. L., Kroner, U., 2016. Phanerozoic Tin and Tungsten Mineralization-Tectonic Controls on the Distribution of Enriched Protoliths and Heat Sources for Crustal Melting. *Gondwana Research*, 31: 60–95.
- Schwartz, M.O., Rajah, S.S., Askury, A.K., et al., 1995. The Southeast Asian Tin Belt. *Earth-Science Reviews*, 38(2–4): 95–293.
- Si, X.B., Sun, X., Xiao, K., et al., 2024. Late Cretaceous Sn Mineralization at Haobadi, Southwestern Yunnan Province, China: Constraints from Cassiterite and Zircon U-Pb Geochronology. *Ore Geology Reviews*, 2105936.
- Söderlund, U., Patchett, P.J., Vervoort, J.D., et al., 2004. The ^{176}Lu Decay Constant Determined by Lu-Hf and U-Pb Isotope Systematics of Precambrian Mafic Intrusions. *Earth and Planetary Science Letters*, 219(3–4): 311–324.
- Sun, X., Deng, J., Lu, L.L., et al., 2023. Temporal and Spatial Distribution of Granite-Associated Tin Deposits and Ore-Forming Process in Southwest Yunnan, China. *Acta Geologica Sinica*, 97(11): 3550–3568 (in Chinese with English abstract).
- Wang, C.M., Bagas, L., Lu, Y.J., et al., 2016. Terrane Boundary and Spatio-Temporal Distribution of Ore Deposits in the Sanjiang Tethyan Orogen: Insights from Zircon Hf-Isotopic Mapping. *Earth-Science Reviews*, 156: 39–65.
- Wang, C.M., Deng, J., Carranza, E.J.M., et al., 2014a. Tin Metallogenesis Associated with Granitoids in the Southwestern Sanjiang Tethyan Domain: Nature, Deposit Types, and Tectonic Setting. *Gondwana Research*, 26(2): 576–593.
- Wang, C.M., Deng, J., Lu, Y.J., et al., 2015a. Age, Nature, and Origin of Ordovician Zhibenshan Granite from the Baoshan Terrane in the Sanjiang Region and Its Significance for Understanding Proto-Tethys Evolution. *International Geology Review*, 57(15): 1922–1939.
- Wang, C.M., Deng, J., Santosh, M., et al., 2015b. Age and Origin of the Bulangshan and Mengsong Granitoids and Their Significance for Post-Collisional Tectonics in the Changning-Menglian Paleo-Tethys Orogen. *Journal of*

- Asian Earth Sciences*, 113: 656–676.
- Wang, D.H., Huang, F., Wang, Y., et al., 2020. Regional Metallogeny of Tungsten-Tin-Polymetallic Deposits in Nanling Region, South China. *Ore Geology Reviews*, 120: 103305.
- Wang, D.Z., Liu, Y.H., Leng, C.B., et al., 2024. Cassiterite and Monazite U-Pb Dating, and Cassiterite Geochemistry of the Shiganghe and Tiechang Tin Deposits in the Baoshan District (NW Yunnan), SW China. *Mineralium Deposita*, 1–23.
- Wang, T., Hou, Z.Q., 2018. Isotopic Mapping and Deep Material Probing (I): Revealing the Compositional Evolution of the Lithosphere and Crustal Growth Processes. *Earth Science Frontiers*, 25(06): 1–19 (in Chinese with English abstract).
- Wang, T., Xiao, W.J., Collins, W.J., et al., 2023. Quantitative Characterization of Orogenes through Isotopic Mapping. *Communications Earth & Environment*, 4(1): 110.
- Wang, W.Q., Dong, G.C., Sun, Z.R., et al., 2021. The Genesis of Eocene Granite-Related Lailishan Tin Deposit in Western Yunnan, China: Constraints from Geochronology, Geochemistry, and S-Pb-H-O Isotopes. *Geological Journal*, 56(1): 508–524.
- Wang, Y.J., Li, S.B., Ma, L.Y., et al., 2015c. Geochronological and Geochemical Constraints on the Petrogenesis of Early Eocene Metagabbroic Rocks in Nabang (SW Yunnan) and Its Implications on the Neotethyan Slab Subduction. *Gondwana Research*, 27(4): 1474–1486.
- Wang, Y.J., Lu, X.H., Qian, X., et al., 2022. Prototethyan Orogenesis in Southwest Yunnan and Southeast Asia. *Scientia Sinica (Terra)*, 52(11): 2077–2104 (in Chinese).
- Wang, Y.J., Xing, X.W., Cawood, P.A., et al., 2013. Petrogenesis of Early Paleozoic Peraluminous Granite in the Sibumasu Block of SW Yunnan and Diachronous Accretionary Orogenesis along the Northern Margin of Gondwana. *Lithos*, 182: 67–85.
- Wang, Y.J., Zhang, L.M., Cawood, P.A., et al., 2014b. Eocene Supra-Subduction Zone Mafic Magmatism in the Sibumasu Block of SW Yunnan: Implications for Neotethyan Subduction and India-Asia Collision. *Lithos*, 206: 384–399.
- Wu F.Y., Guo, C.L., Hu, F.Y., et al., 2023. Petrogenesis of the Highly Fractionated Granites and Their Mineralizations in Nanling Range, South China. *Acta Petrologica Sinica*, 39(01): 1–36 (in Chinese with English abstract).
- Wu, F.Y., Li, X.H., Zheng, Y.F., et al., 2007. Lu-Hf Isotopic Systematics and Their Applications in Petrology. *Acta Petrologica Sinica*, (02): 185–220 (in Chinese with English abstract).
- Xiao, K., Sun, X., Zhang, R.Q., et al., 2024. Cassiterite Geochronology and Geochemistry of the Yunling Sn Deposit: Implication for Late Cenozoic Mineralization in Western Yunnan, China. *Mineralium Deposita*, 1–19.
- Xie, J.C., Zhu, D.C., Dong, G.C., et al., 2016. Linking the Tengchong Terrane in SW Yunnan with the Lhasa Terrane in Southern Tibet through Magmatic Correlation. *Gondwana Research*, 39: 217–229.
- Xu, Y.G., Yang, Q.J., Lan, J.B., et al., 2012. Temporal-Spatial Distribution and Tectonic Implications of the Batholiths in the Gaoligong-Tengliang-Yingjiang Area, Western Yunnan: Constraints from Zircon U-Pb Ages and Hf Isotopes. *Journal of Asian Earth Sciences*, 53: 151–175.
- Yang, J.H., Zhou, M.F., Hu, R.Z., et al., 2020. Granite-Related Tin Metallogenic Events and Key Controlling Factors in Peninsular Malaysia, Southeast Asia: New Insights from Cassiterite U-Pb Dating and Zircon Geochemistry. *Economic Geology*, 115(3): 581–601.
- Yang, T.N., Ding, Y., Zhang, H.R., et al., 2014. Two-Phase Subduction and Subsequent Collision Defines the Paleotethyan Tectonics of the Southeastern Tibetan Plateau: Evidence from Zircon U-Pb Dating, Geochemistry, and Structural Geology of the Sanjiang Orogenic Belt, Southwest China. *GSA Bulletin*, 126(11–12): 1654–1682.
- Yu, L., 2016. Genesis and Tectonic Significance of the Mesozoic Granitoids in the Tengchong-Baoshan Block, Sanjiang Area (Dissertation). China University of Geosciences, Beijing (in Chinese with English abstract).

- Yu, L., Li, G.J., Wang, Q.F., et al., 2014. Petrogenesis and Tectonic Significance of the Late Cretaceous Magmatism in the Northern Part of the Baoshan Block: Constraints from Bulk Geochemistry, Zircon U-Pb Geochronology and Hf Isotopic Compositions. *Acta Petrologica Sinica*, 30(09): 2709–2724, (in Chinese with English abstract).
- Zhang, B., Zhang, J.J., Zhong, D.L., 2010. Structure, Kinematics and Ages of Transpression during Strain-Partitioning in the Chongshan Shear Zone, Western Yunnan, China. *Journal of Structural Geology*, 32(4): 445–463.
- Zhang, Z.Y., Hou, Z.Q., Lü, Q.T., et al., 2023. Crustal Architectural Controls on Critical Metal Ore Systems in South China Based on Hf Isotopic Mapping. *Geology*, 51(8): 738-742.
- Zhao, S.W., Lai, S.C., Pei, X.Z., et al., 2019. Compositional Variations of Granitic Rocks in Continental Margin Arc: Constraints from the Petrogenesis of Eocene Granitic Rocks in the Tengchong Block, SW China. *Lithos*, (326): 125–143.
- Zhao, S.W., Lai, S.C., Qin, J.F., et al., 2014. Zircon U-Pb Ages, Geochemistry, and Sr-Nd-Pb-Hf Isotopic Compositions of the Pinghe Pluton, Southwest China: Implications for the Evolution of the Early Palaeozoic Proto-Tethys in Southeast Asia. *International Geology Review*, 56(7), 885–904.
- Zhao, T.Y., Feng, Q.L., Metcalfe, I., et al., 2017. Detrital Zircon U-Pb-Hf Isotopes and Provenance of Late Neoproterozoic and Early Paleozoic Sediments of the Simao and Baoshan Blocks, SW China: Implications for Proto-Tethys and Paleo-Tethys Evolution and Gondwana Reconstruction. *Gondwana Research*, 51: 193–208.
- Zheng, M.J., Sun, X., Santosh, M., et al., 2024. Triassic Granitic Magmatism in the Lancangjiang Zone in Southwestern China Associated with Paleo-Tethys Evolution and Its Control on Tin Mineralization. *Geological Society of America Bulletin*.
- Zhong, D.L., 1998. The Paleotethys Orogenic Belt in West of Sichuan and Yunnan. Science Publishing House, Beijing, 1–230 (in Chinese).
- Zhu, D.C., Wang, Q., Zhao, Z.D., et al., 2015. Magmatic Record of India-Asia Collision. *Scientific reports*, 5(1): 14289.
- Zhu, R.Z., Lai, S.C., Qin, J.F., et al., 2018. Strongly Peraluminous Fractionated S-Type Granites in the Baoshan Block, SW China: Implications for Two-Stage Melting of Fertile Continental Materials Following the Closure of Bangong-Nujiang Tethys. *Lithos*, 316: 178–198.
- Zhu, R.Z., Lai, S.C., Santosh, M., et al., 2017. Early Cretaceous Na-Rich Granitoids and Their Enclaves in the Tengchong Block, SW China: Magmatism in Relation to Subduction of the Bangong-Nujiang Tethys Ocean. *Lithos*, 286: 175–190.
- Zhu, Y.T., Li, X.F., Li, Z.F., 2022. The Fractures-Controlled Tin Mineralization at the End of Late Cretaceous in the Songshan Deposit, Southwestern China: Constraints from U-Pb Dating of Zircon, Garnet, and Cassiterite. *Ore Geology Reviews*, 150: 105191.

附中文参考文献

- 董美玲, 2013. 滇西保山地块早古生代花岗岩类的地球化学、年代学及其构造意义(硕士学位论文). 北京: 中国地质大学(北京).
- 董美玲, 董国臣, 莫宣学, 等, 2012. 滇西保山地块早古生代花岗岩类的年代学、地球化学及意义. *岩石学报*, 28(05): 1453–1464.
- 杜斌, 王长明, 贺昕宇, 等, 2016. 锆石 Hf 和全岩 Nd 同位素填图研究进展: 以三江特提斯造山带为例. *岩石学报*, 32(08): 2555–2570.
- 侯增谦, 王涛, 2018. 同位素填图与深部物质探测(II): 揭示地壳三维架构与区域成矿规律. *地学前缘*, 25(06): 20–41.
- 胡斌, 2002. 滇西澜沧江成矿带铜成矿学研究(博士学位论文). 湖南: 中南大学.

- 蒋少涌, 赵葵东, 姜海, 等, 2020. 中国钨锡矿床时空分布规律、地质特征与成矿机制研究进展. 科学通报, 65(33): 3730–3745.
- 李海涛, 邵泽东, 2019. 空间插值分析算法综述. 计算机系统应用, 28(07): 1–8.
- 李再会, 林仕良, 从峰, 等, 2012. 滇西腾冲-梁河地块石英闪长岩-二长花岗岩锆石 U-Pb 年龄、Hf 同位素特征及其地质意义. 地质学报, 86(07): 1047–1062.
- 廖世勇, 王冬兵, 唐渊, 等, 2013. “三江”云龙锡(钨)成矿带晚白垩世二云母花岗岩 LA-ICP-MS 锆石 U-Pb 定年及其地质意义. 岩石矿物学杂志, 32(04): 450–462.
- 林进展, 2013. 滇西腾冲锡矿带来利山花岗岩地质地球化学特征与成矿关系分析(硕士学位论文). 北京: 中国地质大学(北京).
- 林进展, 曹华文, 张寿庭, 等, 2015. 青藏高原东南缘腾冲来利山 A 型花岗岩地球化学特征、锆石 U-Pb 定年及其构造意义. 大地构造与成矿学, 39(05): 959–971.
- 陆建军, 朱金初, 刘昌实, 等, 1989. 滇西云龙混合岩及其与锡矿化的关系. 大地构造与成矿学, (03): 264–275.
- 毛景文, 袁顺达, 谢桂青, 等, 2019. 21 世纪以来中国关键金属矿产找矿勘查与研究新进展. 矿床地质, 38(05): 935–969.
- 莫宣学, 2011. 岩浆与岩浆岩: 地球深部“探针”与演化记录. 自然杂志, 33(05): 255–259+313.
- 戚学祥, 韦诚, 蔡志慧, 等, 2019. 滇西腾冲地块高黎贡群变质沉积岩时代与原特提斯洋俯冲/增生: 来自碎屑锆石 U-Pb 定年和岩石地球化学证据. 地质学报, 93(01): 94–116.
- 孙祥, 邓军, 路雷雷, 等, 2023. 滇西南与花岗岩有关的锡矿床时空分布与成矿作用. 地质学报, 97(11): 3550–3568.
- 王涛, 侯增谦, 2018. 同位素填图与深部物质探测(I): 揭示岩石圈组成演变与地壳生长. 地学前缘, 25(06): 1–19.
- 王岳军, 卢向红, 钱鑫, 等, 2022. 滇西-东南亚原特提斯南支的造山作用. 中国科学: 地球科学, 52(11): 2077–2104.
- 吴福元, 郭春丽, 胡方洩, 等, 2023. 南岭高分异花岗岩成岩与成矿. 岩石学报, 39(01): 1–36.
- 吴福元, 李献华, 郑永飞, 等, 2007. Lu-Hf 同位素体系及其岩石学应用. 岩石学报, (02): 185–220.
- 禹丽, 2016. 三江腾冲-保山地块中生代岩浆岩成因及构造意义(博士学位论文). 北京: 中国地质大学(北京).
- 禹丽, 李龚健, 王庆飞, 等, 2014. 保山地块北部晚白垩世岩浆岩成因及其构造指示: 全岩地球化学、锆石 U-Pb 年代学和 Hf 同位素制约. 岩石学报, 30(09): 2709–2724.
- 钟大赉, 1998. 滇川西部古特提斯造山带. 北京: 科学出版社, 1–230.